Acta Crystallographica Section B
Structural Science
ISSN 0108-7681

Structure of the X-phase of 38% brominated betaine calcium chloride dihydrate

L. G. Vieira,[a] O. Hernandez,[b]* J. L. Ribeiro,[a] A. Cousson,[c] J.-M. Kiat,[c,d] M. R. Chaves,[e] A. Almeida[e] and A. Klöpperpieper[f]

[a]Departamento de Física, Universidade do Minho, 4709 Braga codex, Portugal, [b]Laboratoire de Chimie du Solide et Inorganique Moléculaire, UMR 6511 CNRS, Université de Rennes 1, Institut de Chimie de Rennes, Campus de Beaulieu, Avenue du Général Leclerc, 35042 Rennes, France, [c]Laboratoire Léon Brillouin, UMR 12 CNRS-CEA, CEA/Saclay, 91191 Gif-sur-Yvette CEDEX, France, [d]Laboratoire de Structure, Propriétés et Modélisation des Solides, UMR 8580 du CNRS, École Centrale, 92295 Châtenay-Malabry, France, [e]Departamento de Física, Facultade de Ciências da Universidade do Porto, Rua do Campo Alegre 687, 4169-007 Porto, Portugal, and [f]Fachbereich Physik, Universität des Saarlandes, 66041 Saarbrücken, Germany

Correspondence e-mail: olivier.hernandez@univ-rennes1.fr

Received 28 September 2000
Accepted 19 January 2001

The structures of the high- and low-temperature phases of 38% brominated BCCD [betaine (trimethylammonioacetate) calcium chloride dihydrate], the latter being known as the X-phase, have been determined by single-crystal neutron diffraction at 295 and 20 K, respectively. The symmetry of the X-phase is described by the $P2_12_12_1$ space group. The distortion with respect to the high-temperature *Pnma* phase is characterized by anti-symmetric displacements of the betaine molecules as well as of the Ca octahedra. On the basis of a symmetry-mode analysis, we propose an interpretation of the direct phase transition that occurs around 80 K between these two phases.

1. Introduction

The dielectric compound betaine calcium chloride dihydrate [BCCD, $(CH_3)_3NCH_2COOCaCl_2(H_2O)_2$], synthesized in 1984 (Rother *et al.*, 1984), is a noteworthy experimental example of the Devil's staircase concept (Aubry, 1983). Indeed, its thermal phase diagram, between a paraelectric parent phase (space group *Pnma*; Brill *et al.*, 1985; Ezpeleta *et al.*, 1996; above $T_i = 164$ K) and a non-modulated ferroelectric phase (space group $Pn2_1a$; Dernbach, 1993; Ezpeleta *et al.*, 1996; below $T_0 = 46$ K), is constituted by a wealth of one-dimensional displacively modulated phases [$\mathbf{k} = \delta(T)\mathbf{c}^*$], either incommensurate or commensurate (mainly $\delta = \frac{1}{4}, \frac{1}{5}$ and $\frac{1}{6}$ on cooling; Brill & Ehses, 1985; Chaves & Almeida, 1991; Ezpeleta *et al.*, 1996; Schaack & le Maire, 1998).

At room temperature, the orthorhombic unit cell of the parent structure [$a = 10.95\,(1)$, $b = 10.15\,(1)$, $c = 10.82\,(1)$ Å; Ezpeleta *et al.*, 1996] contains four formula units. Each unit constitutes two entities: the polar betaine molecule $[(CH_3)_3N^+CH_2COO^-]$ and a distorted $OOCl_2(H_2O)_2$ octahedron surrounding the Ca atom, which are linked *via* the COO carboxyl terminal group of the betaine molecule (see Fig. 1*a* of Ezpeleta *et al.*, 1996). This structure can be described by a stacking along the *b* axis of parallel layers at $y/b = 1/4$ and $3/4$ (which thus coincide with the *m* mirror plane to which the H2, C1, N, C3, C4, O1 and O2 atoms of the betaine molecule and the Ca atom belong), interconnected along [011] through rather long and anti-symmetric hydrogen bonds between Cl atoms and the water molecules of neighbouring Ca octahedra. Within these layers, the Ca octahedron and the

carboxyl group form quasi-one-dimensional chains directed along the *a* axis, to which the betaine molecules are branched with their axis mainly oriented along the *c* axis. The Ca octahedra belonging to the above-mentioned one-dimensional chains are connected along [100] by Cl···H—O hydrogen bonds, which are nevertheless slightly longer than those between layers (2.288 *versus* 2.248 Å; Ezpeleta *et al.*, 1996).

The structural modulation occurring below T_i is induced by the softening in the parent phase of a mixed optic acoustic phonon mode of Λ_3 symmetry (antisymmetric for C_{2z} and σ_y, symmetric for E and σ_x; Hlinka *et al.*, 1996) and has been studied in detail by Zúñiga *et al.* (1991), Ezpeleta *et al.* (1992) and Hernandez, Quilichini *et al.* (1999). In the incommensurate structure ($T_i > T > 128$ K), the distortion corresponds to a sinusoidal positional modulation with the main displacements directed along the *b* axis. Only the betaine molecule without the carboxyl group behaves as a rigid body with respect to the modulation wave; its modulated motion can be described by a rotation around an axis belonging to the (010) plane and approximately parallel to the connection between the betaine and the Ca octahedron through the O1 atom (Zúñiga *et al.*, 1991). In the fourfold structure ($\delta = 1/4$), the modulation becomes strongly non-sinusoidal and displays for many atoms a two-steps squared shape typical of a soliton regime with respect to the lowest temperature non-modulated ferroelectric structure; nevertheless, the phases of the different atomic modulation functions remain close to those in the incommensurate structure (Hernandez, Quilichini *et al.*, 1999). An extrapolation of these results towards lower temperatures implies similar structures for the successive modulated phases, with greater amplitudes of the distortion and smaller modulation wavenumbers. Finally, the structure of the lowest temperature non-modulated ferroelectric phase ($\delta = 1/\infty$, $T < T_0$) has been studied by Dernbach (1993) and Ezpeleta *et al.* (1996). In this phase the molecular unit loses its mirror plane due essentially to the bending of the rigid part of the betaine molecule and to an antisymmetric displacement of the O1 and O2 atoms.

The phase sequence observed in BCCD can be well described by assuming a single set of irreducible order parameters corresponding to a $\Lambda_3 = B_{3g} + B_{2u}$ modulated distortion, as predicted by Pérez-Mato (1988). Actually, this symmetry of the primary distortion is mirrored in the detected symmetries of the different modulated phases constituting the thermal Devil's staircase: incommensurate phase [$Pnma(00\gamma)0s0$] (Zúñiga *et al.*, 1991), fourfold phase [$P2_1ca$] (Ezpeleta *et al.*, 1992; Hernandez, Kiat *et al.*, 1999), fivefold phase [$P2_12_12_1$] (Hernandez, Kiat *et al.*, 1999), and homogeneous ferroelectric phase [$Pn2_1a$] (Ezpeleta *et al.*, 1996).

The influence of lattice defects in the complex phase sequence observed in pure BCCD has been studied in detail (Schaack & le Maire, 1998). As in other modulated crystals, the presence of lattice defects – either of intrinsic or of extrinsic origin – strongly affects the phase diagram of the compound and induces peculiar thermal hysteresis and non-equilibrium phenomena. These effects, which are related to local symmetry breaking, loss of long-range order and pinning of the soliton lattice, may vary with the nature of defect. In BCCD four types of extrinsic defects have been studied so far: radiation-induced defects (Kiat *et al.*, 1995; le Maire, 1996; le Maire *et al.*, 1997), partial deuteration (Klöpperpieper *et al.*, 1985; Ribeiro *et al.*, 1991*a*; le Maire, 1996), partial replacement of Ca^{2+} by Mn^{2+} (Ribeiro *et al.*, 1991*b*; le Maire, 1996) and partial replacement of Cl^- by Br^- (Ao *et al.*, 1990; Zeitz, 1990; le Maire *et al.*, 1992, 1994, 1997; le Maire, 1996; Vieira *et al.*, 1997; Schaack & le Maire, 1998; Vieira *et al.*, 1998, 1999). Among these, partial bromination has attracted greater attention because this type of defect can be introduced over a wide range of concentrations and affects, in a peculiar way, the phase transition sequence. In fact, as bromine has a larger ionic radius ($r_{Br} = 1.95$ Å) than chlorine ($r_{Cl} = 1.81$ Å), partial bromination induces a local lattice expansion, breaks locally the mirror symmetry of the molecule and alters the delicate balance between intra- and inter-layers couplings which are likely at the origin of the structural modulation in the pure compound.

Several experimental studies in brominated BCCD [$BCCl_{2(1-x)}Br_{2x}D$] have shown that, up to Br concentrations of ~30%, the critical temperatures associated with the onset of the different modulated phases shift towards lower values and the ferroelectric phase is rapidly suppressed (le Maire, 1996; Schaack & le Maire, 1998). These effects reflect essentially the negative chemical pressure induced by the local lattice expansion. Furthermore, for high enough concentrations of bromine, the appearance of a novel non-polar phase is observed (known as the X-phase), stable at low temperature. Actually, as first shown by le Maire (1996), the X-phase is

Table 1
Phase sequence of pure and highly brominated BCCD.

'PE': paraelectric; 'INC': incommensurate; 'COM': commensurate; 'FE': ferroelectric; δ is the modulation wavenumber. For pure BCCD, just the main phases are shown. The temperature range of stability of the phases were taken from Schaack & le Maire (1998). The space groups and superspace group were determined by diffraction methods (Brill *et al.*, 1985; Zúñiga *et al.*, 1991; Ezpeleta *et al.*, 1992; Hernandez, Kiat *et al.*, 1999; Ezpeleta *et al.*, 1996). Highly brominated BCCD: data from Schaack & le Maire (1998), Vieira *et al.* (2000) and the present work.

Phase	Temperature range of stability (K)	(Super-)space group
BCCD		
PE $\delta = 0/1$	>164.0	*Pnma*
INC $0.30 < \delta < 0.32$	127.8–164.0	$Pnma(00\gamma)0s0$
COM $\delta = 2/7$	124.5–127.8	
INC $0.25 < \delta < 0.286$	115.3–125.5	
COM $\delta = 1/4$	75.8–115.3	$P2_1ca$
COM $\delta = 1/5$	53.3–75.2	$P2_12_12_1$
COM $\delta = 1/6$	47.1–53.0	
FE $\delta = 1/\infty$	<46.0	$Pn2_1a$
$BCCl_{2(1-x)}Br_{2x}D$: $x = 0.30$		
PE $\delta = 0/1$	>111	*Pnma*
INC $0.351 < \delta < 0.37$	50–111	$Pnma(00\gamma)0s0$
PE $\delta = 1/\infty$	<50	$P2_12_12_1$
$BCCl_{2(1-x)}Br_{2x}D$: $x = 0.38$		
PE $\delta = 0/1$	>80	*Pnma*
PE $\delta = 1/\infty$	<80	$P2_12_12_1$

Table 2
Experimental details.

	295 K	20 K
Crystal data		
Chemical formula	$C_5H_{11}NO_2{\cdot}CaCl_{1.28}Br_{0.72}{\cdot}2H_2O$	$C_5H_{11}NO_2{\cdot}CaCl_{1.23}Br_{0.77}{\cdot}2H_2O$
Chemical formula weight	296.2	298.4
Cell setting, space group	Orthorhombic, *Pnma*	Orthorhombic, $P2_12_12_1$
a, b, c (Å)	11.02 (3), 10.27 (2), 10.85 (2)	11.04 (3), 10.22 (3), 10.55 (2)
V (Å^3)	1227 (5)	1190 (6)
Z	4	4
D_x (Mg m^{-3})	1.60	1.66
Radiation type	Neutron	Neutron
Wavelength (Å)	1.531	0.8308
No. of reflections for cell parameters	45	37
θ range (°)	11.72–30.06	14.07–26.03
μ (mm^{-1})	0.44	0.45
Temperature (K)	295	20
Crystal form, colour	Cube, colourless	Cube, colourless
Crystal size (mm)	2.0 × 2.0 × 2.0	2.0 × 2.0 × 2.0
Data collection		
Diffractometer	6T2 four-circle	5C2 four-circle
Data collection method	ω, ω–θ and ω–2θ scans	ω scans
No. of measured, independent and observed parameters	3119, 666, 531	2687, 2687, 2275
Criterion for observed reflections	$F^2 > 1\sigma(F^2)$	$F^2 > 3\sigma(F^2)$
R_{int}	0.051	0.058
θ_{max} (°)	49.97	37.92
Range of h, k, l	$-10 \rightarrow h \rightarrow 10$ $-8 \rightarrow k \rightarrow 9$ $-10 \rightarrow l \rightarrow 10$	$0 \rightarrow h \rightarrow 16$ $0 \rightarrow k \rightarrow 15$ $-15 \rightarrow l \rightarrow 3$
No. and frequency of standard reflections	2 every 240 min	1 every 450 min
Refinement		
Refinement on	F	F
R, wR, S	0.0517, 0.0417, 1.0292	0.0508, 0.0405, 1.0715
No. of reflections and parameters used in refinement	531, 151	1569, 253
H-atom treatment	All H-atom parameters refined	All H-atom parameters refined
Weighting scheme	Chebychev polynomial with 5 parameters (Carruthers & Watkin, 1979)	Chebychev polynomial with 3 parameters (Carruthers & Watkin, 1979)
$(\Delta/\sigma)_{max}$	0.079766	0.072778
$\Delta\rho_{max}, \Delta\rho_{min}$ (fm Å^{-3})	0.49, −0.38	1.32, −1.14
Extinction method	Crystallographic Computing [Larson, 1970, eq. (22)]	None
Extinction coefficient	14 (2)	–

already stable at low temperatures in the 24% brominated compound under hydrostatic pressures higher than 50 MPa, and becomes stable even at ambient pressure for higher concentrations of Br ($x = 0.30$ and $x = 0.38$). Table 1 summarizes the phase sequences observed in pure BCCD and in highly brominated crystals ($x = 0.30$ and $x = 0.38$).

Very little is known about the nature of the X-phase, which was firstly evidenced by dielectric constant measurements (le Maire, 1996). Moreover, it turns out that the IR and Raman spectra of the X-phase were found to be different from any of the spectra observed in any phase of pure BCCD (le Maire, 1996; Schaack & le Maire, 1998). More recently, on the basis of optical birefringence and elastic neutron scattering measurements, Vieira *et al.* (2000) have shown that the transition towards the X-phase is of first order, occurs without the appearance of satellite peaks – at least in the (100) plane – and is characterized by a significant decrease of the c parameter and a slight increase of the b parameter.

We present in this paper the structures of the high- and low-temperature phases of 38% brominated BCCD, deduced from neutron diffraction experiments on single crystals. The symmetry of the latter phase – the X-phase – is described by the $P2_12_12_1$ space group. Taking into account the dynamical properties of the pure compound, the transition to the X-phase is discussed on the basis of a symmetry-mode analysis.

2. Experimental

The samples used in this study were of the dimensions $2 \times 2 \times 2$ mm^3 and were cut from the same 38% brominated BCCD single crystal synthesized by slow evaporation from a 70% brominated calcium chloride and betaine aqueous solution.

The neutron diffraction intensities were collected at the Orphée reactor (CEA/Saclay, France) on 6T2 (thermal source) and 5C2 (hot source) four-circle diffractometers at T = 295 and 20 K, respectively. Experimental details are reported in Table 2. We have used as the monochromator crystal vertically bent pyrolitic graphite (002 reflection, *i.e.* λ = 1.531 Å) and copper (220 reflection, *i.e.* λ = 0.8308 Å) on 6T2 and 5C2, respectively. On 6T2 the cylindrical collimators installed on the primary beam, between the monochromator crystal and the sample and between the sample and the detector, were equal to 30, 15 and 25, respectively; on 5C2, only a 58 horizontal collimator was mounted on the incident beam. In order to reduce higher-order contaminations, a pyrolitic graphite filter and an erbium filter was used on 6T2 and 5C2, respectively. The minimum full-width at half maximum was equal to ∼0.2 and 0.4° on 6T2 and 5C2, respectively.

The reduction of the data to F^2_{hkl} values was performed with the *COLL5* program, based on the Lehmann & Larson (1974) algorithm for the 6T2 data and with the *PRON* program (Scherf, 1998) for the 5 C2 data. Both structures were refined

using the *CRYSTALS* program (Watkin *et al.*, 1996), which makes use of the least-squares method. The scattering factors were taken from Sears (1992).

At 295 K, the orthorhombic cell parameters were refined to the following values: a = 11.02 (3), b = 10.27 (2), c = 10.85 (2) Å. The data collection was then performed by ω scans, ω–θ scans and ω–2θ scans in the 2θ range 0–45, 45–80 and 80–120°, respectively. The *Pnma* symmetry of the high-temperature phase of pure BCCD was confirmed. The structure was refined using as a starting model the structure of the latter phase (Ezpeleta *et al.*, 1996). All atoms were refined with anisotropic displacement parameters and an extinction parameter was included once the refinement had converged. The restricted refinement of the occupation parameters of bromine and chlorine sites led to a rate of bromination equal to 0.360 (5).

For the data collection in the X-phase at 20 K, a gas-flow cryostat allowing a thermal stability better than 0.5 K was used. The refined cell parameters [a = 11.04 (3), b = 10.22 (3), c = 10.55 (2) Å] indicated an orthorhombic symmetry within the e.s.d.'s. Several Q-scans performed between Bragg peaks revealed neither superstructure nor satellite reflections. The intensities were then measured by ω scans up to 75° 2θ. The observed systematic extinction rules [(h00): $h = 2n + 1$, (0k0): $k = 2n + 1$, (00l): $l = 2n + 1$] led to the $P2_12_12_1$ space group. The structure of the X-phase was refined using as a starting model the asymmetric unit of the lowest-temperature ferroelectric phase of pure BCCD (Ezpeleta *et al.*, 1996). Non-standard $P2_12_12_1$ symmetry cards (x, y, z; $x+\frac{1}{2}$, $-y+\frac{1}{2}$, $-z+\frac{1}{2}$; $-x$, $y+\frac{1}{2}$, $-z$; $-x+\frac{1}{2}$, $-y$, $z+\frac{1}{2}$) were used so as to maintain the standard origin of the *Pnma* space group of the parent high-temperature phase. The anisotropic displacement parameters of the Cl1 (Br1) and Cl2 (Br2) atoms were set to a single least-squares parameter in order to maintain their values as physically reasonable. The average rate of bromination, 0.386 (8), deduced from the restricted refinement of the occupation parameters of the two inequivalent chlorine/bromine sites, agrees, within 3 e.s.d.'s, with the value obtained at 295 K. The atomic parameters of both phases and geometries have been deposited.[1]

3. Discussion

At room temperature (Fig. 1), the structure of 38% brominated BCCD displays roughly the same features as that of the pure compound (Ezpeleta *et al.*, 1996). In particular, the shape of the individual anisotropic displacement parameters suggests that internal molecular motions particularly tend to twist the methyl groups. In order to specify this point, we have performed a conventional TLS analysis with the *CRYSTALS* program (Watkin *et al.*, 1996). The overall rigid-body motion tensors T, L, S (Schomaker & Trueblood, 1968) have been least-squares fitted to the individual anisotropic displacement parameters. Considering the whole betaine molecule as a rigid-body group leads to an overall R disagreement factor U^{ij} of 0.145 (0.111 without the H atoms), indicating, as expected, that the betaine molecule cannot be considered as a rigid unit. Once the carboxyl group C4O1O2 has been removed from the set of atoms used for the TLS calculation, the R factor for U^{ij} decreases to 0.094 (0.029 without the H atoms), and further to 0.073 for a N—C1H1H2—C2H3H4H5 rigid unit. In the latter case, the diagonal values of the translational T and librational L thermal tensors, with respect to the principal axes of L, are T_{11} = 0.04, T_{22} = 0.06, T_{33} = 0.05 Å^2 and L_{11} = 44.9, L_{22} = 46.3, L_{33} = 177.4 deg^2. The root-mean-square amplitude of the main librational motion (L_{33} term) is therefore equal to 13.3°; the corresponding axis of libration belongs to the (010) plane and is roughly parallel to the C3—C4 bond or to the connection between the betaine and the Ca octahedron through the O1 atom.

On the other hand, due to the fact that bromine has a greater ionic radius than chlorine, two small differences are noticeable between the structures of pure and 38% brominated BCCD at room temperature:

(i) the sites of the Cl and Br atoms do not match exactly, namely both halogens are separated by 0.347 (7) Å;

(ii) the volume of the unit cell increases from 1203 (2) Å^3 in the pure compound (Ezpeleta *et al.*, 1996) to 1227 (5) Å^3 in the 38% brominated crystal.

Moreover, it turns out that the Br···H—O hydrogen bonds, which are the shortest ones in 38% brominated BCCD at 295 K, are (i) stronger than the Cl···H—O bonds in the pure compound; (ii) shorter along [100] (*i.e.* within layers) than along [011] (*i.e.* between layers): 2.199 (9) *versus* 2.23 (1) Å. On the other hand, the Cl···H—O bonds are longer than in the pure compound, but the inter-layer coupling remains stronger than the intra-layer one, contrary to the hydrogen-bond sub-network concerning bromine. It appears that locally, *i.e.* due to the statistical distribution of Cl and Br atoms, the hydrogen-bond network in 38% brominated BCCD is somewhat different from that in pure BCCD, even though on average the balance between inter- and intra-coupling remains unchanged.

In the X-phase at 20 K, the Ca pseudo-octahedron and the betaine molecule are distorted in such a way that their mirror

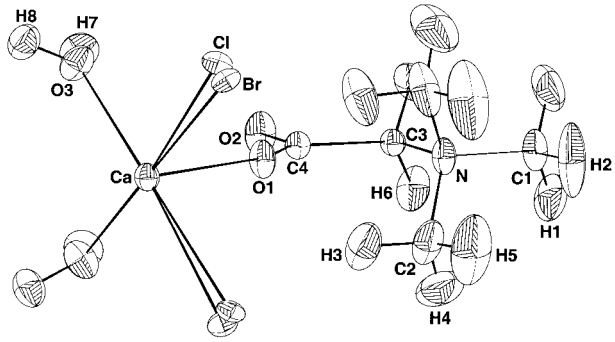

Figure 1
Perspective view of the 38% brominated BCCD molecule at 295 K (displacement ellipsoids represent 20% probability).

[1] Supplementary data for this paper are available from the IUCr electronic archives (Reference: LC0032). Services for accessing these data are described at the back of the journal.

symmetry is broken (see Figs. 2 and 3). More specifically and with respect to their positions in the original molecular mirror plane, the atoms O1 and O2 of the carboxyl group are anti-symmetrically moved, whereas the C3 and C4 atoms remain almost unchanged. For the N and H2 atoms, the distance along **y** between their real sites and the original molecular plane reaches 0.45 and 0.89 Å, respectively. In addition, the distortion of the molecular unit in this phase is associated with the breaking of the *n* and *a* gliding mirror planes of the *Pnma* parent unit cell: the Ca pseudo-octahedra belonging to neighbouring one-dimensional chains, within the layers orthogonal to the *b* axis, librate in opposite directions and the corresponding betaine molecules also bend anti-symmetrically (see Fig. 3). This anti-symmetric libration of the molecules induces a deformation of the diagonal Cl(Br)···H—O hydrogen bonds that link neighbouring octahedra along the [011] direction (Fig. 4). The Cl1—H81 bond length decreases from 2.305 (6) Å at 295 K to 2.211 (7) Å at 20 K, while the Cl2—H82 bond length remains almost constant [2.305 (6) Å at 295 K; 2.306 (6) Å at 20 K]. This deformation together with the bending of the organic groups induces a shrinkage of the unit cell along the *c* axis (Fig. 3), as previously observed (Vieira *et al.*, 2000). Furthermore, within the layers, the Cl···H—O bonds are significantly shortened on cooling [0.09 (1) Å for Cl2—H71], while the Br···H—O bonds are lengthened [0.09 (2) Å for Br2—H71].

The $P2_12_12_1$ space group of the lowest-temperature phase of highly brominated BCCD, 'the X-phase', is a sub-group of *Pnma*, which describes the symmetry of the parent phase of pure as well as of doped BCCD. This simple relationship indicates that the transition towards the X-phase is triggered by an order parameter, which is transformed according to the irreducible representation A_u of the *mmm* point group (anti-symmetric for i, σ_x, σ_y and σ_z).

The study of the low-energy phonon modes of pure BCCD has been carried out by using different experimental techniques. Ao & Schaack (1988) and Volkov *et al.* (1986) used Raman and IR spectroscopies, respectively, to identify low-frequency optical modes (at $q = 0$), with symmetries B_{1g}, B_{3g} and B_{2u}, which are sensitive to temperature from room temperature down to T_i. These modes have been assigned to specific librational degrees of freedom of the betaine and the Ca octahedron. Coherent inelastic neutron scattering experi-

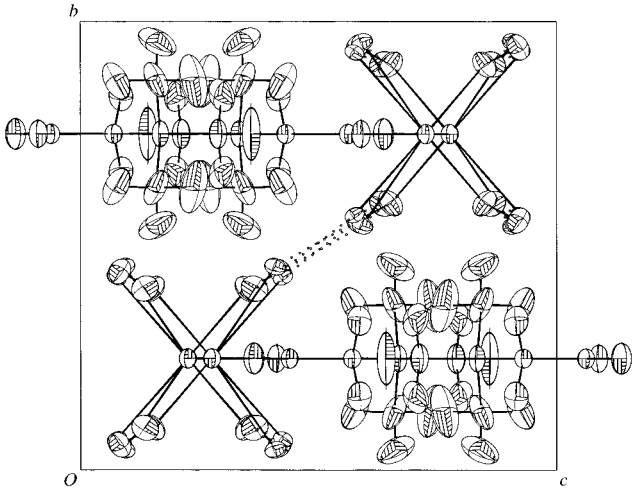

Figure 2
Projection of the unit cell of 38% brominated BCCD on the (100) plane at 295 K. Cl···H—O and Br···H—O hydrogen bonds are indicated. Displacement ellipsoids represent 20% probability.

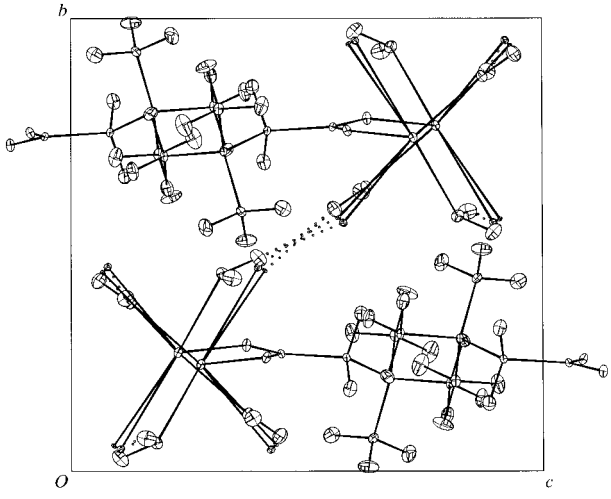

Figure 3
Projection of the unit cell of 38% brominated BCCD on the (100) plane at 20 K. Cl···H—O and Br···H—O hydrogen bonds are indicated. Displacement ellipsoids represent 20% probability.

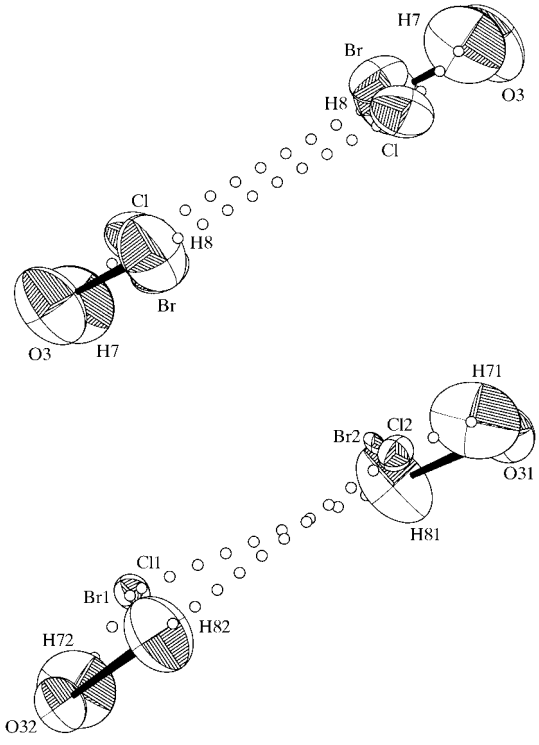

Figure 4
Projection on the (100) plane showing the Cl···H—O hydrogen bonds of 38% brominated BCCD at 295 K (top) and 20 K (bottom). Displacement ellipsoids represent 20 and 50% probability at 295 and 20 K, respectively. For clarity, the Br···H—O hydrogen bonds are not represented.

ments (Hlinka *et al.*, 1996) confirmed the symmetry assignment of these low-energy modes [at $T = 300$ K, $q = 0$: $\nu(B_{2u}) = 0.47$ THz and $\nu(B_{3g}) = 0.675$ THz; $q = c$: $\nu(B_{1g}) = 0.73$ THz] and detected a low-frequency A_u mode [at $T = 300$ K, $q = c$: $\nu(A_u) = 0.39$ THz], which is neither Raman nor IR active. Outside the center of the zone and for $\mathbf{q}//\mathbf{c}^*$, these modes correspond to the symmetries Λ_2 ($B_{1g} + A_u$) and Λ_3 ($B_{3g} + B_{2u}$).

In the parent phase of pure BCCD, the frequencies of the above-mentioned $q = 0$ phonon modes soften when T approaches T_i from above. The lowest frequency A_u mode softens at a rate of the order of $d\nu^2/dT = 0.6 \times 10^{-3}$ THz^2 K^{-1}, while the B_{2u} polar mode softens at a higher rate ($d\nu^2/dT = 1.2 \times 10^{-3}$ THz^2 K^{-1}) (Hlinka *et al.*, 1996). It is therefore this latter B_{2u} mode that induces the onset of the homogeneous ferroelectric phase in the pure compound. On the other hand, it is experimentally known that the inclusion of bromine induces a negative chemical pressure and tends to progressively suppress the ferroelectric and the modulated phases of BCCD. This suggests that bromination increases the frequency of the active B_{2u} mode and/or reduces the rate at which this mode softens. In both cases, the result would be the progressive suppression of the critical instability of the B_{2u} mode and, as a consequence, of the active soft mode responsible for the onset of the modulated phases, which results from the crossing of the B_{2u} optical mode with a transverse acoustic mode (Hlinka *et al.*, 1996). The instability related to the softening of the low-frequency A_u mode, which appears to be less sensitive to bromination, therefore gives rise to the transition towards the non-polar X-phase. Coherent inelastic neutron scattering measurements would be highly desirable to confirm these conclusions.

As in the ferroelectric phase of pure BCCD (Ezpeleta *et al.*, 1996), the distortion of the asymmetric unit of the X-phase with respect to the *Pnma* structure can be described by a libration of the rigid part of the betaine molecule, *i.e.* without the carboxyl group, along an axis roughly parallel to the C3—C4 bond. However, in the case of the X-phase, this distortion is characterized by anti-symmetric displacements of the betaine molecules, as well as of the Ca pseudo-octahedron. The most prominent atomic displacements of the atoms originally in the molecular mirror plane are along the y direction. Besides the primary A_u mode, the A_g mode (the fully symmetric irreducible representation of the *mmm* point group) may contribute to the structural distortion. However, for the eight atoms lying on the molecular mirror plane in the parent structure, there are only three possible symmetry mode contributions: $A_u(y) + A_g(x) + A_g(z)$, where the displacement direction for each mode is indicated within brackets. For these atoms, the fact that the dominant displacements occur along the y direction corresponds therefore to a signature of the symmetry of the primary order parameter.

We are very much indebted to P. Fouilloux and T. Beaufils for their technical support during the experiment on the 6T2 four-circle diffractometer at the Orphée reactor.

References

Ao, R., Lingg, G., Schaack, G. & Zöller, M. (1990). *Ferroelectrics*, **105**, 391–396.

Ao, R. & Schaack, G. (1988). *Ind. J. Pure Appl. Phys.* **26**, 124–130.

Aubry, S. (1983). *Phys. D*, **7**, 240–258.

Brill, W. & Ehses, K. H. (1985). *Jpn J. Appl. Phys.* **24**, 826–828.

Brill, W., Schildkamp, W. & Spilker, J. (1985). *Z. Kristallogr.* **172**, 281–289.

Carruthers, J. R. & Watkin, D. J. (1979). *Acta Cryst.* A**35**, 698–699.

Chaves, M. R. & Almeida, A. (1991). *Geometry and Thermodynamics: Common Problems of Quasi-crystals, Liquid Crystals and Incommensurate Insulators*, edited by J.-C. Tolédano, Vol. 229, pp. 353–369. New York: Plenum Press.

Dernbach, D. (1993). PhD thesis. University of Saarbrücken.

Ezpeleta, J. M., Zúñiga, F. J., Paulus, W., Cousson, A., Hlinka, J. & Quilichini, M. (1996). *Acta Cryst.* B**52**, 810–816.

Ezpeleta, J. M., Zúñiga, F. J., Pérez-Mato, J. M., Paciorek, W. A. & Breczewski, T. (1992). *Acta Cryst.* B**48**, 261–269.

Hernandez, O., Kiat, J.-M., Cousson, A., Paulus, W., Ezpeleta, J. M. & Zúñiga, F. J. (1999). *Acta Cryst.* C**55**, 1463–1466.

Hernandez, O., Quilichini, M., Pérez-Mato, J. M., Zúñiga, F. J., Dŭsek, M., Kiat, J.-M. & Ezpeleta, J. M. (1999). *Phys. Rev. B*, **60**, 7025–7036.

Hlinka, J., Quilichini, M., Currat, R. & Legrand, J.-F. (1996). *J. Phys. Condens. Matter*, **8**, 8207–8219.

Kiat, J.-M., Calvarin, G., Chaves, M. R., Almeida, A., Klöpperpieper, A. & Albers, J. (1995). *Phys. Rev. B*, **52**, 798–802.

Klöpperpieper, A., Rother, H. J., Albers, J. & Müser, H. E. (1985). *Jpn. J. Appl. Phys.* **24**, 829–831.

Larson, A. C. (1970). *Crystallographic Computing*, edited by F. R. Ahmed, S. R. Hall and C. P. Huber, pp. 291–294. Copenhagen: Munksgaard.

Lehmann, M. S. & Larsen, F. K. (1974). *Acta Cryst.* A**30**, 580–584.

Maire, M. le (1996). Ph.D. thesis. University of Würzburg.

Maire, M. le, Lingg, G., Schaack, G., Schmitt-Lewen, M., Strauss, G. & Klöpperpieper, A. (1992). *Ferroelectrics*, **125**, 87–92.

Maire, M. le, López Ayala, A., Schaack, G., Klöpperpieper, A. & Metz, H. (1994). *Ferroelectrics*, **155**, 335–340.

Maire, M. le, Straub, R. & Schaack, G. (1997). *Phys. Rev. B*, **56**, 134–139.

Pérez-Mato, J. M. (1988). *Solid State Commun.* **67**, 1145–1150.

Ribeiro, J. L., Chaves, M. R., Almeida, A., Müser, H. E., Albers, J. & Klöpperpieper, A. (1991*a*). *Phys. Status Solidus B*, **163**, 503–509.

Ribeiro, J. L., Chaves, M. R., Almeida, A., Müser, H. E., Albers, J. & Klöpperpieper, A. (1991*b*). **163**, 511–517.

Rother, H. J., Albers, J. & Klopperpieper, A. (1984). *Ferroelectrics*, **54**, 107–110.

Schaack, G. & le Maire, M. (1998). *Ferroelectrics*, **208–209**, 1–62.

Scherf, C. (1998). *PRON*, revised Stoe version. Institute of Crystallography, Aachen, Germany.

Schomaker, V. & Trueblood, K. N. (1968). *Acta Cryst.* B**24**, 63–76.

Sears, V. F. (1992). *Neutron News*, **3**, 26–37.

Vieira, L. G., Almeida, A., Ribeiro, J. L., Chaves, M. R., Klöpperpieper, A. & Albers, J. (1997). *Phys. Status Solidus B*, **204**, 863–876.

Vieira, L. G., Hernandez, O., Almeida, A., Quilichini, M., Ribeiro, J. L., Chaves, M. R. & Klöpperpieper, A. (1999). *Eur. Phys. J. B*, **10**, 447–456.

Vieira, L. G., Ribeiro, J. L., Almeida, A., Chaves, M. R., Klöpperpieper, A., Albers, J. & Gervais, F. (1988). *Aperiodic '97*, edited by M. de Boissieu, J.-L. Verger-Gaugry and R. Currat, pp. 605–609. Singapore: World Scientific Publishing Co.

Vieira, L. G., Ribeiro, J. L., Hernandez, O., Quilichini, M., Almeida, A., Chaves, M. R. & Klöpperpieper, A. (2000). *Ferroelectrics*, **240**, 169–176.

Volkov, A. A., Goncharov, Y. G., Kozlov, G. V., Albers, J. & Petzelt, J. (1986). *JETP Lett.* **44**, 603–606.

Watkin, D. J., Prout, C. K., Carruthers, J. R. & Betterridge, P. W. (1996). *CRYSTALS*, Issue 10. Chemical Crystallography Laboratory, University of Oxford, England.
Zeitz, A. (1990). Master's thesis. University of Saarbrücken.
Zúñiga, F. J., Ezpeleta, J. M., Pérez-Mato, J. M., Paciorek, W. & Madariaga, G. (1991). *Phase Transit.* **31**, 29–43.